A high-temperature Brillouin scattering study on four compositions of haplogranitic glasses and melts: High frequency elastic behavior through the glass transition

Anwar Hushur[1,2], Murli H. Manghnani[1*], Quentin Williams[3], and Donald B. Dingwell[4]

[1]University of Hawaii, Hawaii Institute of Geophysics and Planetology, Honolulu, HI 96822, USA

[2]Present address: School of Physics Science and Technology, Xinjiang University, Urumqi, 830046, P. R. China

[3]University of California, Department of Earth and Planetary Sciences, Santa Cruz, CA 95064, USA

[4]Earth and Environment, LMU-University of Munich, 80333 Muenchen, Germany

*murli@soest.hawaii.edu

Abstract

The sound velocities (nV_p, V_p, V_s) and refractive index n of four haplogranitic glasses and melts have been measured as a function of temperature by Brillouin scattering spectroscopy. The measurements were conducted at GHz frequency, through the glass transition temperature (T_g), using both platelet and back scattering geometries. The compositions of the four haplogranites are based on the addition of ~5 wt% each of the components Li_2O, F_2O_{-1} and ~9 wt% each of the components of Na_2O, K_2O to a haplogranitic (HPG8) composition. Marked changes in slope and sign are observed in the temperature dependences of sound velocities (nV_p, V_p, V_s) as a function of composition. The glass transition temperatures T_g of the haplogranite samples are determined from distinct slope changes of sound velocities (V_p and V_s) versus temperature. The lithium-enriched glass has the lowest glass transition temperature (466 °C), while the potassic glass has the highest glass transition temperature (575 °C). The unrelaxed bulk moduli vary markedly with composition below the glass transition, as do their temperature dependence: the bulk moduli of the F- and Na-rich glasses have positive shifts with temperature. For comparison, the shear modulus has relatively similar temperature dependences below T_g for different alkali contents. At temperatures above the glass transition, the temperature derivatives of the bulk moduli, which for these frequencies reflect the vibrational compressibilities of the liquids, shift to more negative values. However, the compositional range over which the bulk moduli undergo positive or small negative temperature shifts of the vibrational compressibility appears to extend to NBO/T ratios near 0.3-0.4, or spanning most haplogranite compositions.

Keywords: High Temperature, Elasticity, Brillouin Scattering, Haplogranites

Introduction

Properties such as density, compressibility and viscosity of silicate melts are important in understanding the thermodynamic and fluid dynamic properties of magmatic systems in the Earth's interior. For example, knowledge of the compressibility of silicate melts at ambient pressures has aided in the construction of accurate pressure–volume–temperature equations of state and modeling of thermodynamic properties of magmatic silicate liquids at high pressure (Lange and Carmichael 1990; Ghiorso et al. 2002). Ultrasonic studies have been carried out to determine the sound velocities and compressibility of binary, ternary, and more complex multi-component silicate melts at ambient pressure (Manghnani et al. 1986; Rivers and Carmichael 1987; Kress et al. 1988; Secco et al. 1991b, 1991a; Webb and Dingwell 1994; Webb and Courtial 1996), which show complex temperature and composition dependences of density and compressibility. Moreover, extensive studies have been carried out on the ultrasonic and Brillouin scattering behavior of endmember SiO_2-glass and liquid: these studies have yielded major insight into the relaxational and elastic behavior of pure silica glasses and liquids (Polian et al. 2002; LeParc et al. 2006; Ruffle et al. 2010; Yokoyama et al. 2010). In contrast to these studies on a broad suite of silicate melts and glasses, the elastic behavior of haplogranites as a function of temperature, composition and frequency is not well known. This is despite the fact that these are perhaps the best-investigated silicate melt compositions of geological relevance [e.g., viscosity and viscoelasticity (Dingwell et al. 1992; Dingwell et al. 1993b; Hess et al. 1995; Dingwell et al. 1996; Dingwell et al. 2000; Hess et al. 2001), density (Knoche et al. 1992; Dingwell et al. 1993a; Knoche et al. 1995),

heat capacity (Toplis et al. 2001), surface tension (Bagdassarov et al. 2000) and diffusivities (Chakraborty et al. 1993; Mungall and Dingwell 1997)].

Haplogranites are important model systems for describing the physical state of magmas involved in the petrogenesis of granitic plutons as well as the physics of silicic volcanic eruptions. These melts are also particularly silica-rich. The goal of this study is to characterize the Brillouin spectroscopic properties of a suite of haplogranitic glasses at temperatures extending well into the supercooled liquid regime. Such high-frequency information (if unrelaxed) constrains the vibrational contribution to the compressibility of liquids; static conditions reflect the total compressibility, which is a sum of the configurational and vibrational portions of the compressibility. Thus, the regimes in which we probe these glasses and melts involve both unrelaxed measurements of the glass (a fixed configuration) at ambient and high temperatures, and the relaxed structural configuration of the supercooled liquid sampled at temperatures above the glass transition. The time-scale of our probe is such that the liquids do not have sufficient time to structurally rearrange in response to the probe pulse. Hence, our measurements of supercooled liquids sample the vibrational portion of their compressibility, without the configurational portion of the compressibility.

Haplogranite melts are also useful and well-investigated model systems with respect to phase equilibria, melt structure and thermodynamics. In particular they are well-positioned for investigating the effects of minor amounts of "excess" alkali and alumina on the structure and properties of silica-rich melts (Burnham and Nekvasil 1986). Thus, extensive investigations of temperature, pressure and composition dependences of the molar volume, density, T_g of haplogranite glasses and melts have been carried out

(Dingwell and Webb 1990; Dingwell et al. 1993a; Knoche et al. 1995; Bagdassarov et al. 2004). The addition of trace elements and volatiles to haplogranite glasses and melts has a profound effect on their physical properties, with dramatic lowering of their viscosity, density, glass transition temperature, and melting temperatures. Moreover, the addition of alkali oxides has a large effect on the viscosity of haplogranitic melts. The viscosity decreases with added alkali oxide content in a nonlinear fashion (Hess et al. 1995). As noted above, elasticity data for haplogranitic melts are sparse (Bagdassarov et al. 1993). Yet, detailed knowledge of the elastic behavior of haplogranitic melts as a function of pressure, temperature and chemical composition would be of fundamental importance for the understanding of magmatic processes, and particularly those that involve silicate-rich melts.

Another important aspect of the dynamics of silicate melts is the determination of the response or relaxation time of macroscopic and microscopic melt properties. The glass transition temperature T_g represents, for the observational timescales involved in most determinations of macroscopic properties, the lowest temperature of structural relaxation in silicate melts. At T_g the silicate melt has a viscosity of 10^{12} Pa s, and a relaxation time for shear stresses of about 100 s. Above the glass transition (at longer times and higher temperatures) the silicate melt is a true metastable liquid in local equilibrium with stress and temperature. Thus, that the temperature dependences of Brillouin shifts and acoustic velocity show sharp changes in slope at the glass transition temperature is unsurprising: T_g is the temperature at which the structure of the material begins (on the timescale of the experiment) to alter its configuration in response to temperature. Such breaks in slope of the temperature dependence of the inter-related

properties of elastic constants, acoustic velocities, or Brillouin shifts can be easily used to record T_g (Xu et al. 1992; Askarpour et al. 1993; Duffrène et al. 1998; Polian et al. 2002; Hushur et al. 2005).

Brillouin scattering is inelastic light scattering induced by acoustic phonons. Sound velocity and elastic constants can be determined by measuring the frequency shift of light scattered from the sample. This purely optical technique requires no mechanical contact with the sample and allows experiments on samples of a few tens of microns in dimension, and thus it represents a very convenient method for measuring sound velocities at high temperature and high pressure, where samples must be contained. There are several Brillouin scattering studies on silicate glasses and melts at high temperature and pressure (Xu and Manghnani 1992; Askarpour et al. 1993; Vo-Thanh et al. 1996; Polian et al. 2002; Schilling et al. 2003; Hushur et al. 2005; Tkachev et al. 2005). These studies provide highly useful constraints on both the elastic properties and relaxational characteristics of silicate glasses and melts. These considerations have led us to study elastic properties of haplogranite melts as a function of temperature (through the glass transition) using Brillouin scattering.

Experimental

The Brillouin scattering experiments were conducted on glass samples shaped and polished to $5 \times 4 \times 0.6$ mm^3 thick and mounted on an alumina sample holder. The compositions of the four samples examined are described in Table 1, and are based on ~5 wt% of each of the oxide components Li_2O, F_2O_{-1} and ~9 wt% of each of the oxide components Na_2O, K_2O added to a base of haplogranitic (HPG8) composition. The

samples were investigated by exciting the sample using the 514.5 nm green line of a Spectra Physics Ar ion laser at a beam power of 130 mW (in front of the furnace, = 60 mW). The Brillouin spectroscopic apparatus is described elsewhere (Tkachev et al., 2005). Two Pt-Pt 10% Rh (Type S) thermocouples were used to measure the temperature. One rests slightly against the sample and one is attached to the sample holder. The high temperature Brillouin experiments were performed in a specially designed furnace with four openings for both 90º-platelet and 180º-backscattering geometries (Fig. 1). This enabled continuous monitoring and maintenance of the constancy of the symmetrical platelet geometry of the sample at high temperatures. This was accomplished by monitoring the positions of two reflected beam spots from the sample surface on a screen. During the high temperature measurements on the fluorine- and sodium-enriched glasses (HPG8 F5 and HPG8 Na5), no change in the reflected beam spot positions was observed, indicating that the platelet geometry and symmetrical arrangement of the specimens remained constant. For the lithium-enriched sample (HPG8 Li5), except at 800ºC, the platelet geometry and symmetrical positioning of the specimens also did not change. If the symmetrical platelet geometry of the sample changes during high temperature measurements, the compressional and shear wave velocities cannot be accurately calculated from the Brillouin shift. In contrast, in the case of the high temperature measurements for the potassium-enriched glass (HPG8-K5), the symmetrical arrangement of the sample was observed to be relatively unstable because of the furnace being mechanically disturbed during the experiment, thus changing the geometry and ending that run. For this reason, only data from the backscattering geometry on this sample are given here. Nevertheless, with the exception of the potassic glass, the

159 Brillouin spectra of the haplogranite samples were recorded in both 90º platelet-scattering
160 geometry and backscattering geometry, enabling the calculation of refractive index by
161 comparing the Brillouin shifts measured in two geometries (see below). The Brillouin
162 shifts f_L measured in back scattering geometry are related to the longitudinal sound
163 velocity V_p by

164

$$V_P = \frac{\lambda_o f_L}{2n} \qquad (1)$$

166

167 where n is the refractive index of the sample and λ_o is the wavelength of the
168 incident laser light. Thus, backscattering geometry enables only measurements of nV_p
169 (product of refractive index and longitudinal velocity). The platelet 90º-scattering
170 geometry enables us to measure the sound velocities (V_p and V_s) directly and
171 independently without the knowledge of n (refractive index), according to the relation,

172

173 $$V_{p,s} = \frac{\lambda_o f_{L,T}}{\sqrt{2}} \qquad (2)$$

174 The two scattering geometries thus provide an opportunity to determine the
175 refractive index n of the glasses directly. Because the uncertainties in the frequency shift
176 measurements (better than 0.2%) and the scattering angle (better than 0.2%) were small,
177 the acoustic velocities were determined to better than 1%. For all the high-temperature
178 measurements, the samples were held at every interval for ten minutes at the measured
179 temperature, to assure thermal equilibration of the sample, before spectra were collected.
180 All data were collected as temperature was progressively increased.

181

Results

Typical Brillouin spectra obtained in backscattering and platelet right-angle scattering geometries are shown in Figure 2. We observed only the longitudinal acoustic phonon mode (LA) in backscattering geometry, whereas both the transverse acoustic phonon mode (TA) mode and LA mode are observed in the platelet right-angle scattering geometry. The temperature dependences of Brillouin shifts for HPG8-F5, presented in Figure 3, show that both LA and TA modes do not have simple linear relationships above and below T_g, in contrast to the linear trends reported for basaltic glasses (Schilling et al. 2003). Since the velocity of an acoustic phonon in an isotropic medium (glass) is independent of direction, the refractive index n of the glass can be determined as a function of temperature by taking the ratio of the Brillouin shifts measured in two different geometries at the same temperature. We can also calculate the high temperature density of the glass using the Lorentz-Lorenz expression:

$$(n^2\text{-}1)/(n^2\text{+}2) = 4\pi\alpha\rho/(3M),$$

where M is the molecular weight, α is the electronic polarizability and ρ is the density of the glass. The polarizability, α, is assumed to be constant with temperature. For the cations within the glass, this assumption is likely quite accurate; however, the value of the polarizability of the oxygen anions may weakly increase with temperature (e.g., Yagi and Susa 2003). Hence, our estimated density changes may be weakly overestimated, but any such overestimates are likely to have only a minor effect on our calculated elasticities.

From the values of density ρ, longitudinal V_p and transverse V_s velocities, we calculate the elastic properties of the sample: bulk modulus (K), shear modulus (G), and Poisson's ratio (σ) from:

$$G = \rho V_s^2$$

$$K = \rho V_p^2 - (4/3)G \qquad (3)$$

$$\sigma = (3K - 2G)/2(3K + G)$$

Room temperature densities for all of the investigated samples have been adopted from a previous study of glasses from the same aliquots (Knoche et al. 1995). The elastic properties of these glasses determined in this study at ambient temperature and pressure are listed in Table 2.

Figure 4 shows the temperature-dependent sound velocities (nV_p, V_p, V_s) of the HPG8-Li5 and HPG8-F5 glasses. Marked slope changes are observed in each of the sound velocities at high temperatures (V_p, V_s). These shifts in slope are particularly distinct in the results from the backscattered nV_p measurements, but are present (albeit less sharply resolved) in all results. These discontinuities in slope denote a shift in the structural, and hence relaxational, properties of the liquid. Thus, the glass transition temperature T_g of different haplogranite samples at the GHz frequency of the Brillouin probe can be determined from the change in slope of the temperature-dependent longitudinal or transverse sound velocity. Uncertainties in the value of T_g are ±10 ^{o}C. These mainly resulted from temperature gradients within the furnace (<1 ^{o}C) and uncertainties in determination of the slopes of the velocity measurements above and below T_g.

HPG8-Li5 has the lowest glass transition temperature (466 °C), while HPG8-K5 has the highest glass transition temperature (575 °C) (see Table 2). Our Brillouin results show lower T_g's relative to the reported DSC measurements (Knoche et al. 1995). However, T_g is a kinetic boundary between liquid-like (viscous) and solid-like (elastic) behavior of the glass, and hence is dependent on the rate of heating/cooling of the sample. There are two methods that are commonly deployed to define T_g from heat capacity (C_p) data. First, the temperature at which the peak in the C_p (and/or dV/dT) curve occurs may be used to characterize T_g (Knoche et al. 1995; Stevenson et al. 1995). Second, the temperature at which the extrapolated onset of the rapid increase of C_p occurs can be used to define the T_g (Moynihan 1995; Giordano et al. 2005). The extrapolated onset temperature of the rapid increase of C_p is ~500 °C for the F-bearing haplogranitic glass with ~5 wt% of F_2O_{-1} (Dingwell et al. 1993a), which is very close to our measured T_g in this study. This agreement indicates that the elastically determined T_g in this study corresponds to the extrapolated onset of the rapid increase of C_p in DSC measurements, implying that this characterization of T_g likely provides a more robust determination of T_g than other techniques (Moynihan 1995; Giordano et al. 2005). Indeed, that the Brillouin measurements take a considerable amount of time to set-up, check alignment, and conduct (typically over an hour per data point) indicates that the sample has a considerable amount of time to structurally equilibrate at each temperature. Thus, these measurements are likely to sample a relatively long time-frame/slow-heating rate glass transition relative to other probes, and the expectation is that such T_g's would lie at the low end of previous determinations, as do the onsets of rapid increases in C_p, as opposed to the peaks in heat capacity. In passing, it is important to note that this T_g reflects the

249 internal structural relaxation of the glass/supercooled liquid in response to the change in
250 temperature, and does not refer to relaxation of the glass/supercooled liquid in response
251 to the probe pulse (see below). Here, we refer to the material at temperatures above the
252 glass transition but below the fusion point of the crystalline equivalents as a supercooled
253 liquid: being above the glass transition implies that the material is able to undergo
254 structural/viscous relaxation.

255 The elastic moduli as a function of temperature for three haplogranitic glasses
256 containing Li_2O, Na_2O and F are shown in Figure 5, including the temperature evolution
257 of the unrelaxed bulk and shear moduli, and Poisson's ratio. At temperatures below T_g,
258 both the Na and F-enriched glasses show weakly increasing bulk moduli, which directly
259 reflect the increases in V_p with temperature within these glasses (Fig. 4). This stiffening
260 of the glass as temperature is increased has been observed within SiO_2 and GeO_2 (Polian
261 et al. 2002; LeParc et al. 2006). The microphysical origins of these positive shifts remain
262 unclear, although LeParc et al. (2006) have proposed that it may arise from the thermal
263 annealing of local elastic fluctuations within the glass. Moreover, these shifts may reflect
264 changes in ring statistics, with smaller rings (and narrower Si-O-Si angles) becoming
265 more prevalent at higher temperatures (Geissberger and Galeener 1983; Shimodaira et al.
266 2006).

267 The solid lines in Figure 5 show least-squares fits to the data. For these data,
268 results at temperatures below the glass transition reflect purely the vibrational
269 contribution to the elasticity of the glass; at temperatures above the glass transition,
270 thermally-induced configurational changes occur as the structure of the super-cooled
271 liquid shifts in response to changing temperature. However, the relaxation time of the

liquid itself is far longer than that of the ~10^{-10} second timescale of the Brillouin probe. Maxwell's relation between relaxation time, shear modulus and viscosity yields a relaxation time of ~2 seconds for the Na5 glass near 600 °C, which decreases to ~3 x 10^{-4} seconds at our highest temperatures of 1123 K [using viscosity data from Hess et al. (1995) and our determination of the shear modulus]. While these estimates are for the shear relaxation time, volumetric relaxation times in liquid silicates have generally been viewed as comparable in length to shear relaxation times (e.g., Bhatia 1967; Kress et al. 1989; Dingwell and Webb 1990). Hence, the liquid is unable to configurationally respond on the time-frame of the probe pulse, as demonstrated by the propagation of shear waves through the liquid sample. Thus, our results above the glass transition represent moduli that are vibrationally relaxed on materials with thermally equilibrated configurations, but which are configurationally unrelaxed with respect to the transient stress change induced by the probe pulse.

The bulk and shear moduli and Poisson's ratio show significant compositional variations at ambient temperature. On heating, the bulk moduli show markedly different temperature dependences (including differences in sign) below T_g with different alkali contents, while the shear moduli G show relatively similar temperature dependences below T_g with different alkali contents (Fig. 5). The Poisson's ratios of HPG8-Li5 and HPG8-F5 glasses increase monotonically in the measured temperature range, while the Poisson's ratio of HPG8-Na5 shows a minimum at 135 °C. The anomalous increases at temperatures up to T_g of the bulk modulus of both the sodium- (above 135 °C) and fluorine-bearing samples likely are generated by the same structural behavior that produces such behavior in end-member silica glass: a temperature-induced narrowing of

the Si-O-Si (or T-O-T) angles, accompanied by a decreased compressibility/increased bulk modulus at high temperatures (e.g., Shimodaira et al. 2006). The more normal negative derivative of the bulk modulus with temperature of the Li-bearing glass may be associated with a higher degree of depolymerization of this glass relative to the Na- and F-bearing glasses (the role of F may be to enhance the degree of polymerization of the silicate glass: Mysen et al. 2004). We speculate that the initially negative slope of the bulk modulus of the Na-bearing glass between 25 and 135 °C, and the higher temperature slope reversal, might reflect a trade-off between the response of the depolymerized/Na-sites within the glass (that may dominate at lower temperature) and a higher temperature predominance of the response of the silicate network. The detailed temperature-dependent *K*, *G* and Poisson's ratio are presented below.

HPG8-Li5:

Both *K* and *G* decrease with increasing temperature; however, their temperature dependences below and above T_g are different, and the Poisson's ratio increases steadily with temperature. The least-squares fits to the data give the following linear equations for *K*, *G* and Poisson's ratio:

Shear modulus *G*:

Below T_g: $32.20(4)-0.00328(13)\times T$; Above T_g: $36.19(20)-0.01201(32)\times T$

Bulk modulus *K*:

Below T_g: $43.13(7)-0.00076(23)\times T$; Above T_g: $48.20(29)-0.0116(5)\times T$

Poisson's ratio: $0.19997(58)+0.000026(1)\times T$

318

319 HPG8-Na5:

320 The bulk modulus initially decreases with increasing temperature, reaches a
321 minimum at ~ 135 °C, increases up to T_g, and then reverses sign and shows a distinct
322 negative temperature dependence. The $(\partial K / \partial T)$ slope changes from -0.0043(18) GPa/°C
323 below 135 °C to 0.0040(5) GPa/°C between 135 °C and T_g. The Poisson's ratio also
324 shows a minimum at around 135 °C. The best least-squares fit to the data gives the
325 following linear equations for *K*, *G* and Poisson's ratio:

326 Shear modulus *G*:

327 Below T_g: 30.34(11)-0.00097(40)×*T*; Above T_g: 33.05(38)-0.0058(5)×*T*

328 Bulk modulus *K*:

329 Below 130°C: 39.72(15)-0.0043(18)×T; Below T_g: 38.71(15)+0.0040(5)×T

330 Above T_g: 42.34(57)-0.0031(8)×*T*

331

332 Poisson's ratio:

333 Below 130°C: 0.198(2)-0.000054(27)×*T,* Above 130°C 0.1904(13)+0.000027(2)×*T*

334

335 HPG8-F5:

336 The bulk modulus shows a marked positive temperature dependence below T_g,
337 and a very small temperature dependence above T_g. The shear modulus *G* shows a slight
338 positive temperature dependence below T_g, and a distinct negative temperature
339 dependence above T_g. The Poisson's ratio increases steadily with increasing temperature.

The best least-squares fit to the data gives the following linear equations for K, G and Poisson's ratio:

Shear modulus G:

Below T_g: 27.73(5)+0.00078(18)×T; Above T_g: 31.47(27)-0.0060(4)×T

Bulk modulus K:

Below T_g: 35.59(6)+0.0063(2)×T; Above T_g: 38.74(19)+0.00007(30)×T

Poisson's ratio: 0.19114+0.000033×T

The behavior of the elastic constants above the glass transition is also worthy of note. The absolute values of the temperature dependences of both K and G just above T_g remain relatively small for both the Na- and F-enriched liquids (Fig. 5). Usually, in a liquid, increasing the temperature changes not only the average interatomic spacing but also the short-range order. This in turn typically leads to a stronger temperature dependence in the moduli of liquids above T_g.

From a broader perspective, the elastic moduli of the three materials shown in Figure 5 are quite similar to one another at temperatures above about 600 °C, being separated from one another by little more than 1.5 GPa in both their bulk and shear moduli. At lower temperatures, the stiffness of the glasses decreases strongly in the order Li>Na>F; the larger value for Li relative to Na is in accord with the smaller and less compressible character of the Li ion, while that of F can likely be attributed to the effect of introducing the relatively compressible F-ion into the amorphous network. However,

363 at temperatures akin to those of granite petrogenesis, at least the absolute value of the
364 vibrational component of the compressibility of these supercooled liquids is nearly
365 independent of composition.

366 **Discussion**

367 Figure 6(a,b) shows correlations between the temperature derivatives of the
368 elastic moduli of these liquids (divided by the absolute value of the moduli) and the
369 thermal expansion of these materials above and below their glass transition, as
370 determined by Knoche et al. (1995). Our Brillouin measurements probe the elasticity
371 associated with fixed positions of the (vibrating) atoms within the glass, and their
372 thermally relaxed positions (which do not configurationally relax during our probe)
373 within the super-cooled liquids. Therefore, it is anticipated that the temperature
374 dependence of the vibrational moduli will depend on the temperature-dependent shifts in
375 the volume of the material, with higher thermal expansions associated with larger
376 temperature-induced decreases in the moduli. Figure 6 confirms this expectation: those
377 glasses with the lowest thermal expansions tend to have either smaller or more positive
378 temperature derivatives of the moduli relative to the corresponding super-cooled liquids.
379 Notably, the ratio of the two axes of Figure 6a define the adiabatic thermodynamic
380 function, δ_S (known as the Anderson-Grüneisen parameter), of the different materials
381 (e.g., Barron 1979). This key measure of anharmonicity is defined as –
382 $(\mathrm{d}\ln K_S/\mathrm{d}T)/\alpha$ where α is the thermal expansion, or equivalently as $-(\mathrm{d}\ln K_S/\mathrm{d}\ln V)_P$. This
383 parameter is typically viewed as roughly constant for crystals and generally lies between
384 ~2.5 and 5 (e.g., Anderson et al. 1991). However, it clearly varies dramatically across the
385 glass-supercooled liquid transition, and adopts values that range from –9.4 for the

386 fluorinated haplogranite glass to a reasonably normal value of 3.4 for the Li-supercooled
387 liquid. This marked variation is a direct consequence of the anomalous positive pressure
388 (or small negative) pressure shifts of the elastic parameters.

389 *Comparison with, and Possible Extension to, Static Elastic Values*

390 The relationship between the relaxed and unrelaxed moduli represents a critical
391 uncertainty in Brillouin spectra of glasses and supercooled liquids. Indeed, the strength of
392 volumetric versus shear relaxational mechanisms is not well-constrained within silicates,
393 although there are indications within water-rich liquids that volumetric relaxational
394 mechanisms (and hence relaxational effects on the bulk modulus) may be substantially
395 weaker than shear relaxational mechanisms (Halalay and Nelson 1992; Tkachev et al.
396 2005). However, a general estimate of the static compressibility of haplogranitic liquids
397 can be made, by utilizing the parameters fit by Lange and Carmichael (1987) to the
398 compressibility of a wide range of compositions of silicate liquids. For the haplogranite
399 that is enriched in sodium by ~9 wt%, we derive a bulk modulus at 1673 K of 13.5 GPa;
400 using the temperature derivatives associated with Lange and Carmichael's (1987) partial
401 molar compressibilities, an estimated bulk modulus of 15.2 GPa at 1073 K can be derived.
402 Thus, thermal corrections induce about a 12% change in compressibility over this
403 temperature interval. In accord with the Brillouin measurements not sampling
404 configurational contributions to the compressibility, our data yield a substantially larger
405 high frequency bulk modulus of 39 GPa for this composition at 1073 K. Therefore, the
406 difference between the static (zero frequency) bulk modulus inferred from Lange and
407 Carmichael (1987) combined with our high-frequency modulus implies that the
408 vibrational contribution to the compressibility comprises about 39% of the total

409 compressibility of this glass, with the balance being produced by configurational effects.
410 This can be compared with end-member silica, for which the vibrational contribution to
411 the total compressibility is near 25% (Bucaro and Dardy 1974; Polian et al. 2002). Hence,
412 the possibility exists that depolymerization may reduce the dominant role of
413 configurational effects on the compressibility of silicate liquids.

414 That the configurational compressibility may play a larger role in more
415 polymerized melts is also indicated by the temperature derivatives of the compressibility
416 of liquids as a function of polymerization. Figure 7 shows the dependence of $d\ln K_s/dT$ of
417 a suite of silica-rich super-cooled liquids as a function of their *NBO/T* ratio. In effect, this
418 illustrates the compositional range over which the anomalous positive temperature
419 derivative of the vibrational bulk modulus (increasing stiffness with increased
420 temperature) of silica disappears and reaches more normal values. The canonical
421 interpretation for this positive temperature derivative involves a narrowing of the average
422 Si-O-Si angle with increasing temperature, and production of three- and four-membered
423 rings of tetrahedra within the supercooled liquid at high temperatures (Geissberger and
424 Galeener 1983; LeParc et al. 2006; Shimodaira et al. 2006). Previously, results on
425 quenched glasses at temperatures up to the glass transition on the Na_2O-SiO_2 binary have
426 indicated that the dependence on composition of the elasticity of annealed glasses
427 changes in slope at a composition near an NBO/T ratio of 0.44 (Vaills et al. 2001).

428 Our results, combined with other Brillouin spectra on supercooled liquids,
429 indicate that: (1) the effect of alkalis (and depolymerization) is to markedly reduce the
430 anomalous elastic behavior associated with shifts in ring statistics in silica and silica-rich
431 supercooled liquids; (2) the onset of 'normal' elastic behavior (as defined by negative

temperature derivatives of elastic parameters) probably commences near an NBO/T ratio of ~0.3; and (3) haplogranites reside in a compositional range where anomalous effects associated with temperature-dependent changes in ring statistics are important for their elastic properties. Hence, depending on their degree of hydration, the well-documented anomalous elastic properties of SiO_2-endmember liquids could extend to granitic magmas.

Acknowledgments

This work was supported by the National Science Foundation (Grants EAR 05-38884 and 09-57137). We thank John Balogh for maintaining our high-temperature Brillouin scattering facility at the University of Hawaii. The haplogranite samples were fabricated in Dingwell´s laboratories in research supported primarily by the Deutsche Forschungsgemeinschaft and Freistaat Bayern. SOEST and Hawaii Institute of Geophysics and Planetology contribution No. xxxx.

References

Anderson, O. L., Isaak, D.L., and Oda, H. (1991) Thermoelastic parameters for six minerals at high temperature. Journal of Geophysical Research, 96, 18037-18046, doi: 10.1029/91jb01579.

Askarpour, V., Manghnani, M.H. and Richet P. (1993) Elastic properties of diopside, anorthite, and grossular glasses and liquids - A Brillouin scattering study up to 1400 K. Journal of Geophysical Research, 98, 17683-17689.

Bagdassarov, N., Dorfman, A., and Dingwell D.B. (2000) Effect of alkalis, phosphorus, and water on the surface tension of haplogranite melt. American Mineralogist, 85, 33-40.

Bagdassarov, N.S., Dingwell D.B., and Webb S.L. (1993) Effect of boron, phosphorus and fluorine on shear-stress relaxation in haplogranite melts. European Journal of Mineralogy, 5, 409-425.

Bagdassarov, N.S., Maumus, J., Poe, B., Slutskiy, A.B., and Bulatov, V.K. (2004) Pressure dependence of T_g in silicate glasses from electrical impedance measurements. Physics and Chemistry of Glasses, 45, 197-214.

Barron, T.H.K. (1979) A note on Anderson-Grüneisen functions. Journal of Physics C-Solid State, 12, L155-L159.

Bhatia, A.B. (1967) Ultrasonic Absorption. 427 pp., Dover Press, New York.

Bucaro, J.A., and Dardy H.D. (1974) High-temperature Brillouin scattering in fused quartz. Journal of Applied Physics, 45, 5324-5329, doi: 10.1063/1.1663238.

468 Burnham, C.W., and Nekvasil H. (1986) Equilibrium properties of granite pegmatite
469 magmas. American Mineralogist, 71, 239-263.
470 Chakraborty, S., Dingwell, D.B., and Chaussidon M. (1993) Chemical diffusivity of
471 boron in melts of haplogranitic composition. Geochimica et Cosmochimica Acta,
472 57, 1741-1751.
473 Dingwell, D.B., and Webb, S.L. (1990) Relaxation in silicate melts. European Journal of
474 Mineralogy, 2, 427-449.
475 Dingwell, D.B., Knoche, R., Webb, S.L., and Pichavant M. (1992) The effect of B_2O_3 on
476 the viscosity of haplogranitic liquids. American Mineralogist, 77, 457-461.
477 Dingwell, D.B., Knoche, R., and Webb S.L. (1993a) The effect of F on the density of
478 haplogranite melt, American Mineralogist, 78, 325-330.
479 Dingwell, D.B., Knoche, R., and Webb S.L. (1993b) The effect of P_2O_5 on the viscosity
480 of haplogranitic liquid. European Journal of Mineralogy, 5, 133-140.
481 Dingwell, D.B., Romano, C., and Hess, K.U. (1996) The effect of water on the viscosity
482 of a haplogranitic melt under P-T-X conditions relevant to silicic volcanism.
483 Contributions to Mineralogy and Petrology, 124, 19-28.
484 Dingwell, D.B., Hess, K.U., and Romano, C. (2000) Viscosities of granitic (sensu lato)
485 melts: Influence of the anorthite component. American Mineralogist, 85, 1342-
486 1348.
487 Duffrène, L., Gy, R., Masnik, J.E., Kieffer, J., and Bass, J.D. (1998) Temperature
488 dependence of the high-frequency viscoelastic behavior of a soda-lime-silica glass.
489 Journal of the American Ceramic Society, 81, 1278-1284.

Geissberger, A.E., and Galeener, F.L. (1983) Raman studies of vitreous SiO_2 versus fictive temperature, Physical Review B, 28, 3266-3271.

Ghiorso, M.S., Hirschmann, M.M., Reiners, P.W., and Kress III, V.C., (2002) The pMELTS: A revision of MELTS for improved calculation of phase relations and major element partitioning related to partial melting of the mantle to 3 GPa. Geochemistry, Geophysics, Geosystems, 3, 1030, doi: 10.1029/2001gc000217.

Giordano, D., Nichols, A.R.L., and Dingwell, D.B. (2005) Glass transition temperatures of natural hydrous melts: a relationship with shear viscosity and implications for the welding process. Journal of Volcanology and Geothermal Research, 142, 105-118, doi: 10.1016/j.jvolgeores.2004.10.015.

Halalay, I.C., and Nelson, K.A. (1992) The liquid--glass transition in $LiCl/H_2O$: Impulsive stimulated light scattering experiments and mode-coupling analysis. Journal of Chemical Physics, 97, 3557-3572, doi: 10.1063/1.462990.

Hess, K.U., Dingwell, D.B., and Webb, S.L. (1995) The influence of excess alkalis on the viscosity of a haplogranitic melt. American Mineralogist, 80, 297-304.

Hushur, A., Kojima, S., Kodama, M., Whittington, B., Olesiak, M., Affatigato, M., and Feller, S.A. (2005) Elastic anomaly of glass transitions in lithium silicate. Japanese Journal of Applied Physics, 44, 6683-6687.

Knoche, R., Webb, S.L., and Dingwell, D.B. (1992) A partial molar volume for B_2O_3 in haplogranitic melt. Canadian Mineralogist, 30, 561-569.

Knoche, R., Dingwell, D.B., and Webb S.L. (1995) Melt densities for leukogranites and granitic pegmatites - partial molar volumes for SiO_2, Al_2O_3, Na_2O, K_2O, Li_2O,

Rb_2O, Cs_2O, MgO, CaO, SrO, BaO, B_2O_3, P_2O_5, F_2O_{-1}, TiO_2, Nb_2O_5, Ta_2O_5, and WO_3. Geochimica et Cosmochimica Acta, 59, 4645-4652.

Kress, V.C., Williams, Q., and Carmichael, I.S.E. (1988) Ultrasonic investigation of melts in the system Na_2O-Al_2O_3-SiO_2. Geochimica et Cosmochimica Acta, 52, 283-293, doi: 10.1016/0016-7037(88)90084-1.

Kress, V.C., Williams, Q., and Carmichael, I.S.E. (1989) When is a silicate melt not a liquid? Geochimica et Cosmochimica Acta, 53, 1687-1692, doi: 10.1016/0016-7037(89)90253-6.

Lange, R.A., and Carmichael, I.S.E. (1987) Densities of Na_2O-K_2O-CaO-MgO-FeO-Fe_2O_3-Al_2O_3-TiO_2-SiO_2 liquids: New measurements and derived partial molar properties. Geochimica Cosmochimica Acta, 51, 2931-2946.

Lange, R.A., and Carmichael, I.S.E. (1990) Thermodynamic properties of silicate liquids with emphasis on density, thermal expansion and compressibility. Reviews in Mineralogy and Geochemistry, 24, 25-64.

LeParc, R., Levelut, C., Pelous, J., Martinez, V., and Champagnon B. (2006) Influence of fictive temperature and composition of silica glass on anomalous elastic behaviour. Journal of Physics: Condensed Matter, 18, 7507-7527.

Manghnani, M.H., Sato, H., and Rai, C.S. (1986) Ultrasonic velocity and attenuation measurements on basalt melts to 1500 ^oC - Role of composition and structure in the viscoelastic properties. Journal of Geophysical Research, 91, 9333-9342.

Moynihan, C.T. (1995), Structural relaxation and the glass transition. Reviews in Mineralogy and Geochemistry, 32, 1-19.

Mungall, J.E., and Dingwell, D.B. (1997) Actinide diffusion in a haplogranitic melt: Effects of temperature, water content, and pressure. Geochimica et Cosmochimica Acta, 61, 2237-2246, doi: 10.1016/s0016-7037(97)00084-7.

Mysen, B.O., Cody, G.D., and Smith, A. (2004) Solubility mechanisms of fluorine in peralkaline and meta-aluminous silicate glasses and in melts to magmatic temperatures. Geochimica et Cosmochimica Acta, 68, 2745-2769, doi: 10.1016/j.gca.2003.12.015.

Polian, A., Vo-Thanh, D., and Richet, P. (2002), Elastic properties of α-SiO_2 up to 2300 K from Brillouin scattering measurements, Europhysics Letters, 57, 375-381.

Rivers, M.L., and Carmichael I.S.E. (1987) Ultrasonic studies of silicate melts. Journal of Geophysical Research, 92, 9247-9270, doi: 10.1029/JB092iB09p09247.

Ruffle, B., Ayrinhac, S., Courtens, E., Vacher, R., Foret, M., Wischnewski, A., and Buchenau, U. (2010). Scaling the temperature-dependent boson peak of vitreous silica with the high-frequency bulk modulus derived from Brillouin scattering data. Physical Review Letters, 104, 067402, doi: 10.1103/PhysRevLett.104.067402.

Schilling, F.R., Sinogeikin, S.V., Hauser, M., and Bass, J.D. (2003) Elastic properties of model basaltic melt compositions at high temperatures. Journal of Geophysical Research, 108, doi: 10.1029/2001JB000517.

Secco, R.A., Manghnani, M.H., and Liu, T.C. (1991a), The bulk modulus - attenuation - viscosity systematics of diopside-anorthite melts. Geophysical Research Letters, 18, 93-96.

Secco, R.A., Manghnani, M.H., and Liu, T.C. (1991b) Velocities and compressibilities of komatiitic melts. Geophysical Research Letters, 18, 1397-1400.

Shimodaira, N., Saito, K., Sekiya, E.H., and Ikushima, A.J. (2006), Microscopic structural changes of SiO_2 glasses as a function of temperature investigated by in situ Raman spectroscopy, Physical Review B, 73, 214206.

Stevenson, R.J., Dingwell, D.B., Webb, S.L., and Bagdassarov, N.S. (1995) The equivalence of enthalpy and shear-stress relaxation in rhyolitic obsidians and quantification of the liquid-glass transition in volcanic processes. Journal of Volcanology and Geothermal Research, 68, 297-306.

Tkachev, S.N., Manghnani, M.H., Williams, Q., and Ming, L.C. (2005) Compressibility of hydrated and anhydrous Na_2O-$2SiO_2$ liquid and also glass to 8 GPa using Brillouin scattering. Journal of Geophysical Research, 110, B07201, doi: 10.1029/2004JB003328.

Toplis, M.J., Gottsmann, J., Knoche, R., and Dingwell, D.B. (2001) Heat capacities of haplogranitic glasses and liquids. Geochimica et Cosmochimica Acta, 65, 1985-1994.

Vaills, Y., Luspin, Y., and Hauret, G. (2001) Annealing effects in SiO_2-Na_2O glasses investigated by Brillouin scattering. Journal of Non-Crystalline Solids, 286, 224-234, doi: 10.1016/s0022-3093(01)00523-3.

Vo-Thanh, D., Polian, A., and Richet, P. (1996) Elastic properties of silicate melts up to 2350 K from Brillouin scattering. Geophysical Research Letters, 23, 423-426.

Webb, S., and Courtial, P. (1996) Compressibility of melts in the CaO-Al_2O_3-SiO_2 system. Geochimica et Cosmochimica Acta, 60, 75-86.

Webb, S.L., and Dingwell, D.B. (1994) Compressibility of titanosilicate melts. Contributions to Mineralogy and Petrology, 118, 157-168.

Xu, J., Manghnani, M.H., and Richet, P. (1992) Brillouin-scattering studies of $K_2Si_4O_9$ glass and melt up to 1000 ^oC. Physical Review B, 46, 9213-9215.

Xu, J., and Manghnani M.H. (1992) Brillouin-scattering studies of a sodium-silicate glass in solid and melt conditions at temperatures up to 1000 ^oC. Physical Review B, 45, 640-645.

Yagi, T., and Susa, M. (2003) Temperature dependence of the refractive index of Al_2O_3-Na_2O-SiO_2 melts: Role of electronic polarizability of oxygen controlled by network structure. Metallurgical and Materials Transactions B, 34B, 549-554.

Yokoyama, A., Matsui, M., Higo, Y., Kono, Y., Irifune, T., and Funakoshi, K.-I. (2010) Elastic wave velocities of silica glass at high temperatures and high pressures. Journal of Applied Physics, 107, 123530-123535, doi: 10.1063/1.3452382.

Figure Captions

TABLE 1. ICP-AES chemical compositions of the four anhydrous haplogranite samples (wt%). Standard deviations are given in parenthesis.

TABLE 2. Ambient density, non-bridging oxygens ratio, elasticity, and glass transition temperature of HPG8 system. Standard deviations are given in parenthesis.

Figure 1. Cross-section of the high temperature furnace used for Brillouin spectroscopy. Two Pt-Pt 10% Rh (Type S) thermocouples were used to measure the temperature. One rests slightly against the sample and one is attached to the sample holder.

Figure 2. A typical Brillouin spectrum measured in (a) right-angle scattering geometry and (b) back scattering geometry. LA indicates the longitudinal acoustic phonon, while TA is the transverse acoustic phonon.

Figure 3. Brillouin shift of HPG8-F5 as a function of temperature measured in two scattering geometries. Errors on the measurements are shown by the error bars within the symbols

Figure 4. Sound velocity (nV_p, V_p, V_s) of (a) HPG8-Li5 (b) HPG8-F5 (c) HPG8-Na5 (d) HPG8-K5 as a function of temperature. Errors on the measurements are shown by the error bars within the symbols; for nV_p, the errors are typically smaller than the size of the symbol. For V_s and V_p, errors tend to be slightly larger than the symbols.

Figure 5. Elastic moduli and Poisson's ratio (calculated from the V_p and V_s measurements) versus temperature for three haplogranite glasses. Errors on the measurements are shown by the error bars within the symbols. The solid lines are

linear least-squares fits to the data above and below the glass transition, with the exception of the sodium-enriched glass below 135 °Ç, which is fit separately, as it shows a different trend.

Figure 6a (left). Logarithmic derivative with respect to temperature of the vibrational bulk modulus as a function of the thermal expansion of glasses and liquids; thermal expansions are from Knoche et al. (1995) and reflect the thermal expansion of the glass at 400 °C and that of the liquid at 50 °C above the glass transition temperature. Error bars on both thermal expansions and the logarithmic derivatives are either less than, or comparable to, the size of the symbols. Lines are drawn to illustrate the shift in elasticity and thermal expansion on passing through the glass transition. Figure 6b (right). Comparable diagram to (a) for changes in the temperature dependence of the shear modulus across the glass transition.

Figure 7. Dependence of the logarithmic derivative of the bulk modulus on the ratio of the number of non-bridging oxygens to tetrahedral cations for supercooled liquids, as determined from high-temperature Brillouin spectroscopy. The results for SiO_2, $K_2Si_4O_9$ and a soda-lime silica composition are from Polian et al. (2002), Xu et al. (1992) and Duffrene et al. (1998), respectively. The fluorinated composition is not included as the effect of fluorine on melt polymerization is not straightforward [e.g., Mysen et al. (2004)].

TABLE 1. ICP-AES chemical compositions of the four anhydrous haplogranite samples (wt%). Standard deviations are given in parenthesis.

Oxide Composition (wt%)	HPG8_Li05	HPG8_Na05	HPG8_K05	HPG8_F05
SiO_2	73.2(3)	74.1(4)	74.6(8)	77.0(2)
Al_2O_3	12.9(3)	11.7(6)	11.8(8)	11.1(1)
Na_2O	4.3(3)	9.0(2)	4.4(8)	4.5(1)
K_2O	4.4(2)	4.4(9)	9.2(10)	4.1(1)
Li_2O	4.9(4)	0.000	0.000	0.000
F	0.000	0.000	0.000	4.6(1)
Total	99.7	99.2	100.0	101.3

TABLE 2. Ambient density, non-bridging oxygens ratio, elasticity, and glass transition temperature of HPG8 system. Standard deviations are given in parenthesis.

	Density (g/cm^3)	NBO/T	n	nV_p	V_p	V_s	K	G	Poisson's ratio	T_g^* (°C)	T_g^{**} (°C)
HPG8_Li05	2.3667	0.209	1.498	9.03(2)	6.03(5)	3.69(3)	43.0(4)	32.2(3)	0.201(2)	513	466 (10)
HPG8_Na05	2.3766	0.105	1.481	8.58(2)	5.79(5)	3.56(3)	39.7(4)	30.0(3)	0.198(2)	595	529 (10)
HPG8_K05	2.3645	0.072	1.478	8.46(2)	5.721(5)	3.54(3)	37.9(4)	29.6(3)	0.190(2)	639	575 (10)
HPG8_F05	2.3003		1.442	8.22(2)	5.70(5)	3.48(3)	37.6(4)	27.8(3)	0.204(2)	584	508(10)

NBO/T: (non-bridging oxygens)/(tetrahedrally coordinated cations)

$^*T_g$: Determined at 5 K/min using the peak value of C_p by differential scanning calorimetry (Knoche et al. 1995).

$^{**}T_g$: Determined by Brillouin spectroscopy.

Figures

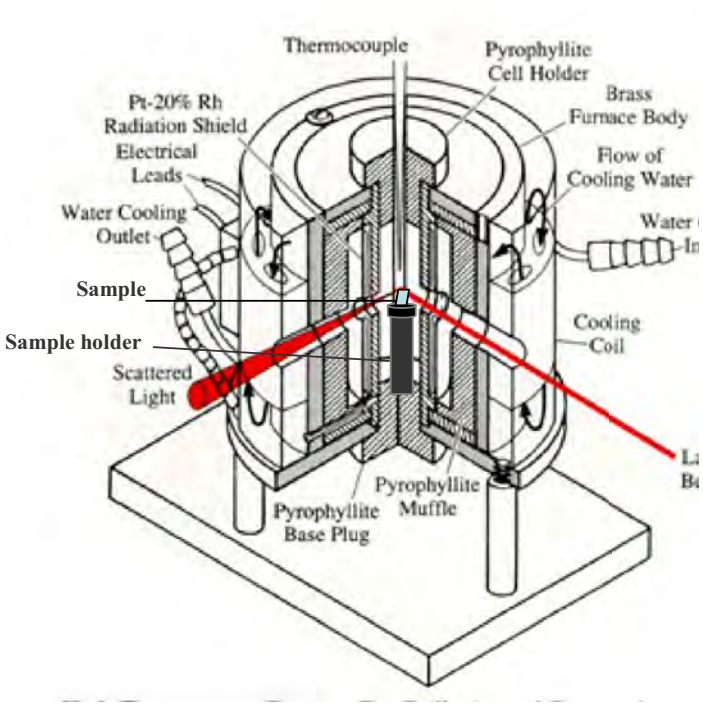

Figure 1. Cross-section of the high temperature furnace used for Brillouin spectroscopy. Two Pt-Pt 10% Rh (Type S) thermocouples were used to measure the temperature. One rests slightly against the sample and one is attached to the sample holder.

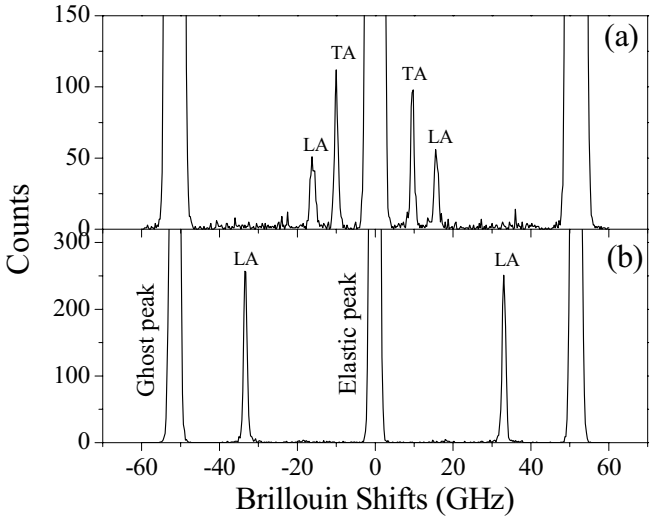

Figure 2. A typical Brillouin spectrum measured in (a) right-angle scattering geometry and (b) back-scattering geometry. LA is longitudinal acoustic phonon. TA is transverse acoustic phonon.

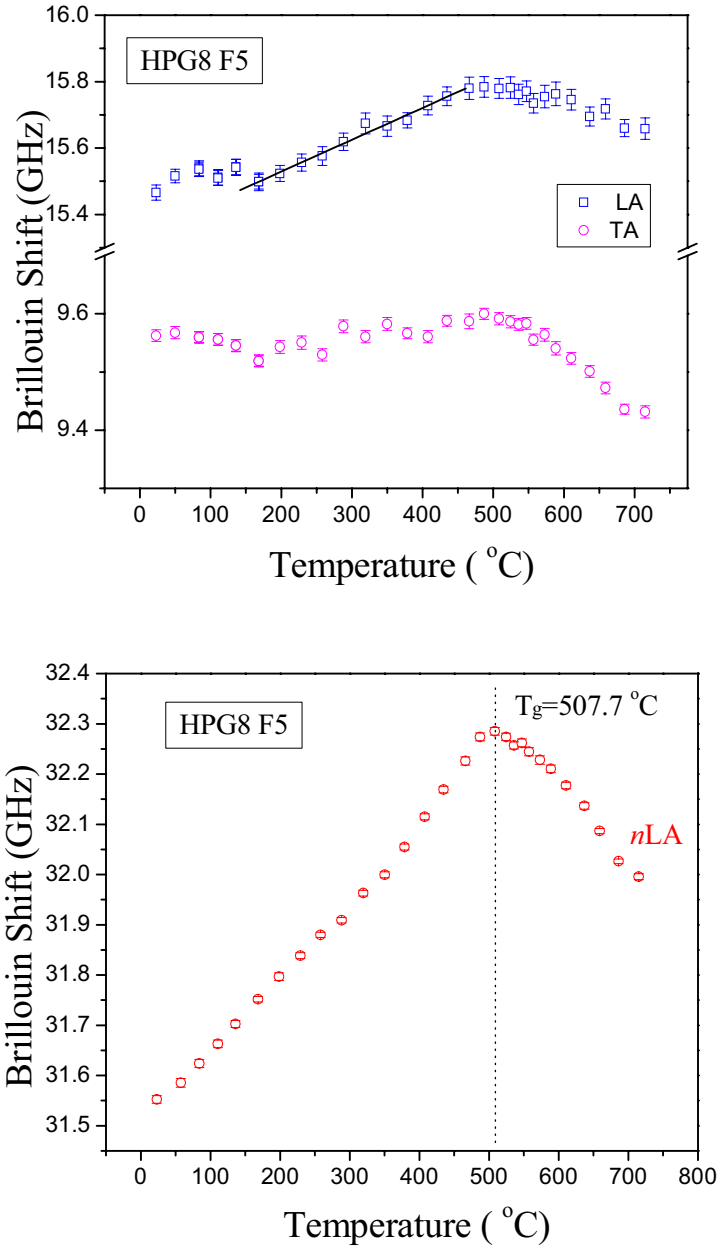

Figure 3. Brillouin shift of HPG8-F5 as a function of temperature measured in two scattering geometries.

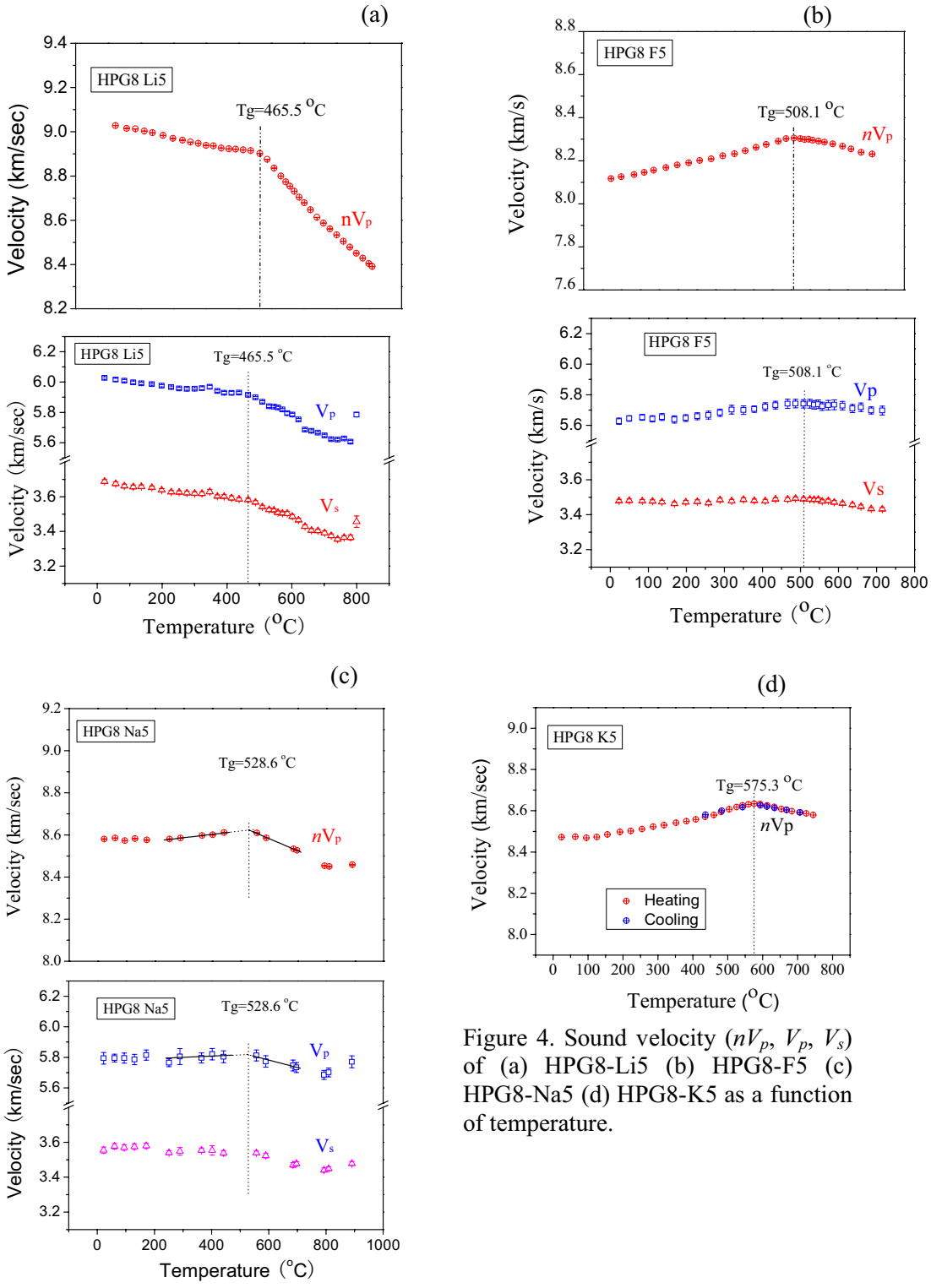

Figure 4. Sound velocity (nV_p, V_p, V_s) of (a) HPG8-Li5 (b) HPG8-F5 (c) HPG8-Na5 (d) HPG8-K5 as a function of temperature.

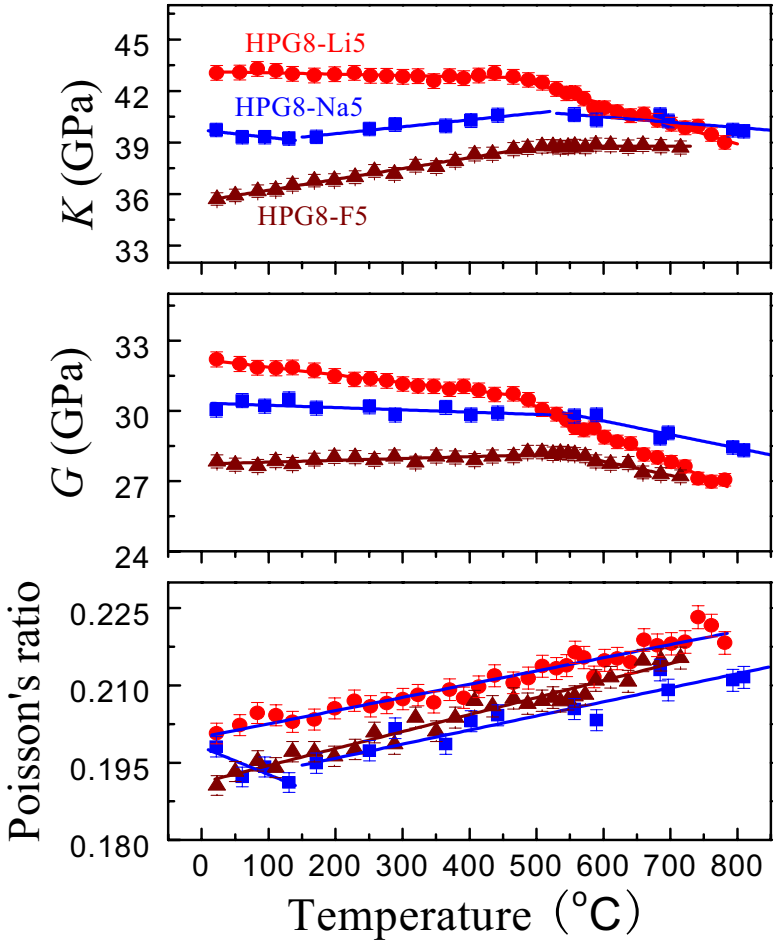

Figure 5. Elastic moduli and Poisson's ratio (calculated from V_p, V_s and ρ) versus temperature for three haplogranite glasses. The solid lines are least-squares fits to the data above and below the glass transition in each respective sample.

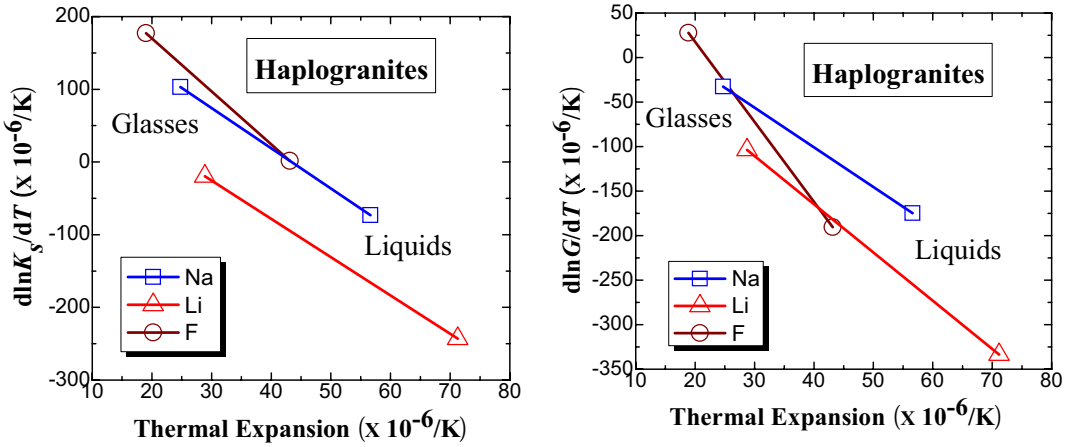

Figure 6a (left). Logarithmic derivative with respect to temperature of the vibrational bulk modulus as a function of the thermal expansion of glasses and liquids; thermal expansions are from Knoche et al. (1995) and reflect the thermal expansion of the glass at 400 °C and that of the liquid at 50 °C above the glass transition temperature. Error bars on both thermal expansions and the logarithmic derivatives are either less than, or comparable to, the size of the symbols. Lines are drawn to illustrate the shift in elasticity and thermal expansion on passing through the glass transition. Figure 6b (right). Comparable diagram to (a) for the temperature dependence of the shear modulus.

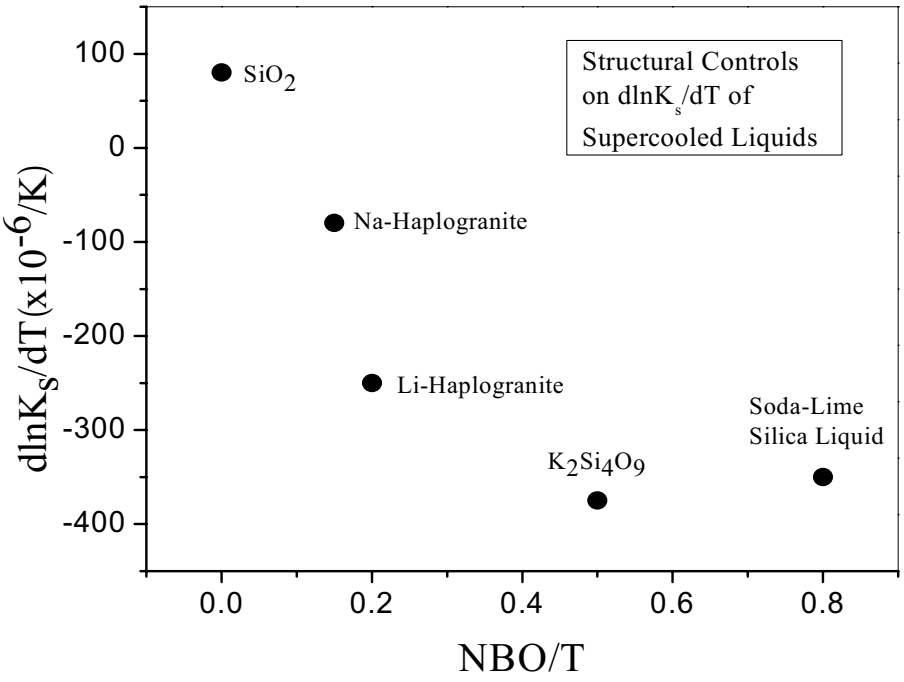

Figure 7. Dependence of the logarithmic derivative of the bulk modulus on the ratio of the number of non-bridging oxygens to tetrahedral cations for supercooled liquids, as determined from high-temperature Brillouin spectroscopy. The results for SiO_2, $K_2Si_4O_9$ and a soda-lime silica composition are from Polian et al. (2002), Xu et al. (1992) and Duffrene et al. (1998), respectively. The fluorinated composition is not included as the effect of fluorine on melt polymerization is not straightforward (e.g., Mysen et al. 2004).